Applied Solid Mechanics Summative

Sheila Shafira

Part A: FEA Investigation and Report

Executive Summary

This report summarises the structural analysis of a lug that will be attached to the Gas Combustion Unit (GCU) for Liquified Natural Gas (LNG) carriers. Finite Element Analysis was done using Abaqus CAE to investigate stress and deflection of the lifting lug and to evaluate the suitability of the lug geometry for the application. The material used for this component is S355JR Structural Steel. It was found that the maximum Von Mises' stress outside the contact region is 179.6 MPa and the vertical deflection at the tip is 0.128 mm. To ensure the relevance of the analysis, it was then validated by analytical solution of simplified designs and by conducting mesh convergence study.

Material Properties and Loading

The lug will be fabricated from S355JR Structural Steel as agreed in the proposal. This structural steel has the following properties: Young's Modulus of 209 GPa, Poisson's ratio of 0.3, Yield strength of 355 MPa, Ultimate Tensile Strength of 630 MPa, elongation at failure of 22%, and density of 8010 kg/m^3 [1].

To simplify the analysis, there are several assumptions regarding the loading condition. It is assumed that the GCU system will be lifted at a constant speed, and the overall mass of the GCU is distributed equally between 6 lugs. A concentrated force of 58,860 N was found using equation (1). This value was used during the analysis as the force exerted on the lug.

$$P = \frac{m\,g}{6} \tag{1}$$

Where P is the total load (N), m is the overall mass of the GCU which is 36,000 kg and g is the acceleration of gravity which is 9.81 ms^{-2}.

FE Analysis

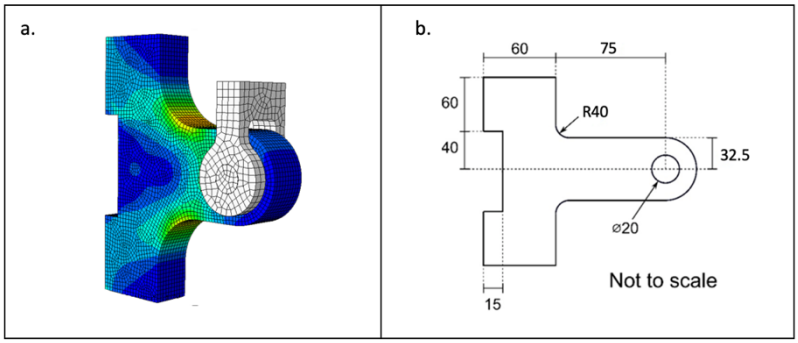

Figure 1: a.) FEA model of the lug design and the pin and shackle. b.) Dimensions (in mm) of the lug model

The geometry of the lug is shown in figure 1(b), it has a uniform thickness of 30 mm. The analysis was done by modelling a lifting shackle on the lug, as shown in figure 1(a). The lifting shackle and pin was modelled to make the analysis as realistic as possible to real life practice. The pin and shackle are modelled as rigid bodies to simplify the analysis, therefore it is assumed that these components do not deform. The vertical faces of the lug is fixed for all translational degrees-of-freedom as it will be welded to the GCU. The lug and pin are also constrained in all degrees-of-freedom with the exception of vertical displacement. Contact interactions with tangential and normal friction of coefficient of 0.2 was specified as the 3

components; lug, pin and shackle will be interacting with each other. The analysis was done in 3 steps; the initial step when the boundary conditions are created, second step is applying small uniform pressure of magnitude 0.001 to the top face of the shackle, and the last step is applying the full load, which is a concentrated force of 58,860 N acting upward applied at the top of the lifting shackle, where it propagates by pulling the pin and exerts force directing upward on the lug hole. The model was meshed with quadratic tetrahedral elements with adaptive mesh of global seed size 10.

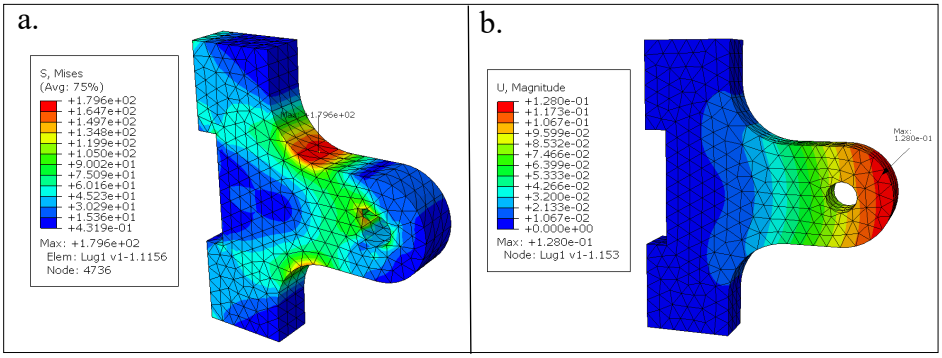

Figure 2 a.) Von Mises' Stress. b.) Displacement

The maximum Von Mises' stress (excluding the contact region) was found to be 179.6 MPa, located at the neck of the lug, and the tip displacement was found to be 0.128 mm. To validate the analysis, the result was then compared to analytical solution and by doing mesh convergence study.

FE Validation

Contact Theory

To validate the pin and shackle model, the FE result was compared to an analytical solution using bearing stress equation, a particular case of contact mechanics [2]. It was assumed that the contact forces from the pin acts normal to tangent of the contact surface which is the inner diameter of the lug hole. It was also assumed that it has negligible clearance and that the pin was rigid. This results on an assumption where load is uniformly distributed, therefore equation (2) was used.

$$\sigma_b = \frac{4}{\pi}\frac{F}{L \times D} \tag{2}$$

Where σ_b is the bearing stress in MPa, F is the radial load of 58,860 N, D was diameter of the pin which was 20 mm, and L was the pin and inner hole contact length which was 30 mm. It was assumed that the contact area is the upper half surface of the lug hole. This equation gives the result of 124.9 MPa. It was found during the analysis that there is stress singularity in the contact area, where maximum stress does not converge, therefore, the analytical value is compared to the pressure exerted by the pin on the lug hole, which is the stress at vertical direction with the value of 134.7 MPa, which has an error of 7% compared to the analytical solution.

Timoshenko-Ehrenfest Beam Theory

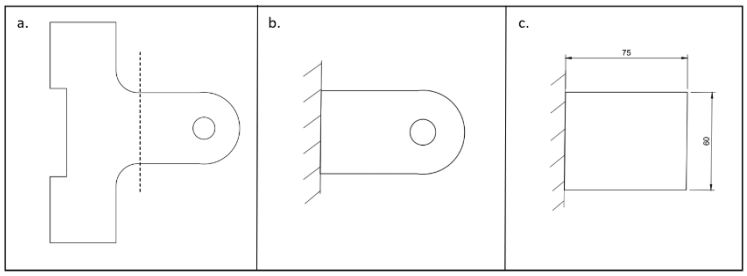

Figure 3 Timoshenko beam model

To validate tip displacement result, it is compared to Timoshenko beam theory that is applicable to short beams. This theory considers the shear deformation and rotational bending effect. For this validation, the lug was modelled as a thick cantilever beam with rectangular cross-section.

$$\delta_{tip} = \frac{PL^3}{3EI} + \frac{PL}{kGA} \qquad (3)$$

Equation (3) was used to find tip displacement, where P is the total load of 58,860 N, L is the length of the beam which is 75 mm, E is the Young's Modulus which is 209 GPa, I is the second moment of inertia of a rectangular cross-section which is 686,562.5 m^4, k is the ratio of displacement which in this case was 5/6, G is the shear modulus of 80,384.6 MPa and A was the cross-sectional area which is 1950 mm^2. It was obtained that the displacement at the tip was 0.09 mm. This gives 40% error compared to FE result of 0.128 mm. This caters or the fact that this beam model is extremely simplified. However, both results are in the same order of magnitude, thus this analytical result can be used as a sanity check.

Mesh Convergence Study

To develop an adequate but efficient FEA model, mesh convergence study was conducted. To determine the appropriate element type and size, the analysis was done with hexahedral element and tetrahedral element with adaptive remeshing rule, resulting in variable mesh sizes with finer mesh at higher stress region. Both element types are of quadratic orders, ensuring more accurate result compared to linear when it comes to capturing curved edges [5]. Convergence study for both elements was done by running the simulation with coarse mesh, then simulating the same model with finer mesh. All results were normalized to the value predicted by the coarse mesh.

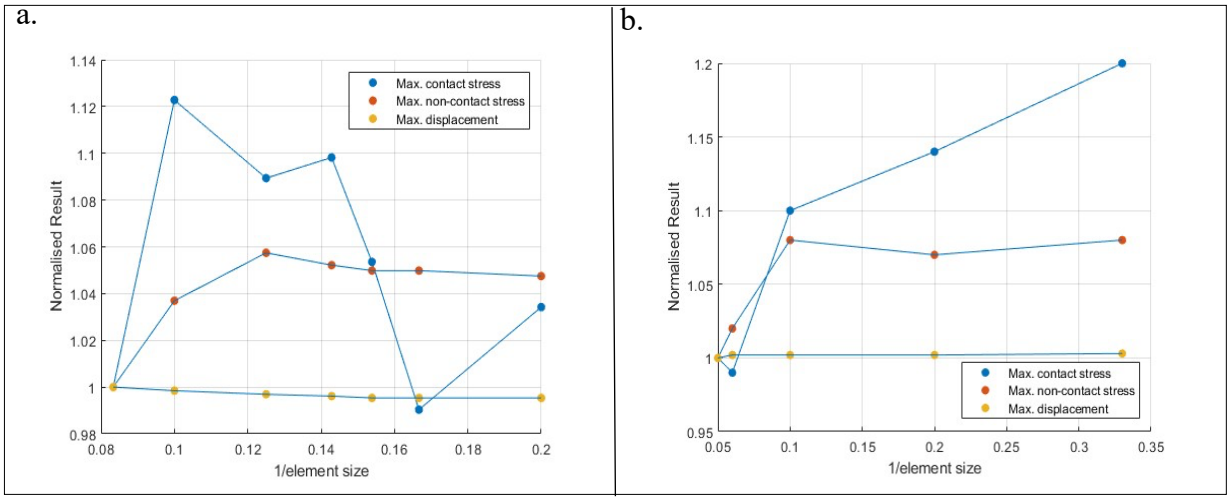

Figure 4 a.) Hexahedral element. b.) Tetrahedral element.

When looking at maximum Von Mises stress result at non-contact region shown in figure 4, it was found that tetrahedral element converges faster at mesh size of 10 while hexahedral element converges at size 7. It was found that stress converges much later than displacement, this happens because stress and strain are calculated using displacement gradient, therefore finer mesh is required to predict displacement gradient than is needed to predict displacement. It was also found that there is stress singularity at the contact region of pin and lug hole, resulting in the stress result not converging at that region. It was concluded from the study that tetrahedral elements of size 10 provides an accurate result. This was also validated by obtaining the error between element of size 10 and 5, which results in negligible error of 3%. This ensures the relevance of the analysis as mesh independence is reached.

Design Evaluation

The finite element analysis provides useful insight to this lifting lug design. However, there are several limitations to this analysis as assumptions were made. Analysis for different loading regime needs to be done since the FE simulation was only done in a scenario where the applied force was normal to the tangent of lug hole surface and the load was distributed equally. The pin and shackle were also idealized as rigid bodies whilst in real life they will experience deformations. There was also stress singularity at the contact region. Theoretically, stress is infinite at the location, resulting in non-converging mesh. Sub modelling for this specific region is required to provide accurate result [3], as the contact region is a critical region where various failure mechanism can occurs. Refinement to the design can also be done by refining the lug geometry. Further analysis can be done to ensure the safety of the design for the application by modelling the response of materials in the plastic regime to multiaxial loading, which is a more complex and deep analysis compared to this design which was done for linear-elastic material only.

References

1. Harry Coules & Alexander Velichko, 07/11/2022, MENG 30011 Applied Solid Mechanics, AY 2022/23 coursework assessment, University of Bristol.

2. Bearing pressure (2022) Wikipedia. Wikimedia Foundation. Available at: https://en.wikipedia.org/wiki/Bearing_pressure#:~:text=Bearing%20pressure%20is%20a%20particular%20case%20of%20contact,such%20as%20a%20plastic%20deformation%20similar%20to%20peening. (Accessed: December 10, 2022).

3. Mesh convergence (2004) Getting started with Abaqus/Standard: Keywords Version (V6.5-1). ABAQUS, Inc. Available at: https://classes.engineering.wustl.edu/2009/spring/mase5513/abaqus/docs/v6.5/books/gss/default.htm?startat=ch04s04.html (Accessed: December 10, 2022).

4. Dion *et al*. (1969) *Solving timoshenko beam equation for cantilever beam*, *Engineering Stack Exchange*. Available at: https://engineering.stackexchange.com/questions/48965/solving-timoshenko-beam-equation-for-cantilever-beam (Accessed: December 11, 2022).

5. The Analyst (2022) Linear vs quadratic fe elements, FEA Tips. Available at: https://featips.com/2019/03/29/linear-vs-quadratic-fe-elements/ (Accessed: December 11, 2022).

6. *Abaqus CAE - Finite element modeling, visualization, and process automation*. Available at: https://www.3ds.com/products-services/simulia/products/abaqus/abaquscae/

Part B: Theory of FEA

1. a.) 66 elements
   b.) 46 nodes
   c.) 46 x 2 = 92 degrees-of-freedom

2. The element stiffness matrix can be found using the coordinates of the triangle and the material properties.

Table 1: Coordinates of the constant strain triangle

Nodes	Coordinates
1	(0.58,-3.42)
2	(0.18,-1.74)
3	(-1.00,-3.31)

It is a linear-elastic and isotropic material in plane stress with the Young's Modulus (E) of 166 GPa and Poisson's Ratio (v) of 0.29.
For a constant strain triangle (CST), the element stiffness matrix can be found using the following equation:

$$\boldsymbol{K} = \iiint_V \boldsymbol{B}^T(\boldsymbol{r})\boldsymbol{D}\boldsymbol{B}(\boldsymbol{r})dV(\boldsymbol{r}) = \Delta \boldsymbol{B}^T\boldsymbol{D}\boldsymbol{B} \tag{1}$$

All the terms in this equation are known material properties and $\boldsymbol{B}^T\boldsymbol{D}\boldsymbol{B}$ is constant for CST. First, Δ was obtained by plugging in the CST coordinates.

$$\Delta = \frac{[(x_2y_3 - x_3y_2) + (x_3y_1 - x_1y_3) + (x_1y_2 - x_2y_1)]}{2} \tag{2}$$

The value of Δ was obtained to be 1.305. Then we compute the transpose of $\boldsymbol{B}$ using equation (3) and we obtain equation (4):

$$\boldsymbol{B} = \frac{1}{2\Delta}\begin{pmatrix} y_2 - y_3 & 0 & y_3 - y_1 & 0 & y_1 - y_2 & 0 \\ 0 & x_3 - x_2 & 0 & x_1 - x_3 & 0 & x_2 - x_1 \\ x_3 - x_2 & y_2 - y_3 & x_1 - x_3 & y_3 - y_1 & x_2 - x_1 & y_1 - y_2 \end{pmatrix} \tag{3}$$

$$\boldsymbol{B}^{\mathrm{T}} = \begin{pmatrix} 1.0246 & 0 & -0.7701 \\ 0 & -0.7701 & 1.0246 \\ 0.0718 & 0 & 1.0311 \\ 0 & 1.0311 & 0.0718 \\ -1.0964 & 0 & -0.2610 \\ 0 & -0.2610 & -1.0964 \end{pmatrix} \tag{4}$$

Then we compute $\boldsymbol{D}$, where for isotropic material in plane stress can be computed using equation (5).

$$\boldsymbol{D} = \frac{E}{1 - v^2}\begin{pmatrix} 1 & v & 0 \\ v & 1 & 0 \\ 0 & 0 & (1 - v)/2 \end{pmatrix} \tag{5}$$

Substituting the results from equation (2), (3),(4) and (6) we then obtain the stiffness matrix to be:

$$\mathbf{K} = 10^{11} \times \begin{pmatrix} 2.9813 & -1.2039 & -0.4928 & 0.6783 & -2.4885 & 0.5255 \\ -1.2039 & 2.2844 & 0.8493 & -1.8166 & 0.3546 & -0.4678 \\ -0.4928 & 0.8493 & 0.9050 & -1.8166 & -0.4122 & -0.9622 \\ 0.6783 & -1.8166 & 0.1129 & 0.1129 & -0.7913 & -0.7028 \\ -2.4885 & 0.3546 & -0.4122 & -0.4122 & 2.9007 & 0.4367 \\ 0.5255 & -0.4678 & -0.9622 & -0.9622 & 0.4367 & 1.1706 \end{pmatrix} \text{ N/m} \quad (6)$$

3. Equation (7) shows the relation of stiffness matrix **K** and nodal forces **f**.

$$\mathbf{f} = \mathbf{K}\,\mathbf{u} \quad (7)$$

In matrix form:

$$\begin{pmatrix} f_{1x} \\ f_{1x} \\ f_{2x} \\ f_{2y} \\ f_{3x} \\ f_{3y} \end{pmatrix} = \mathbf{K} \begin{pmatrix} u_{1x} \\ u_{1y} \\ u_{2x} \\ u_{2y} \\ u_{3x} \\ u_{3y} \end{pmatrix} \quad (8)$$

Where **K** is equation (6).
Node 2 and 3 are constrained in both directions, giving 0 displacements, therefore the last 4 rows can be discarded as the terms are multiplied by 0. f_{1x} and f_{1y} are known, with the values of 66.0 MN/m and 83.9 MN/m respectively. This leaves us with equation (9), where we solve u_{1x} and u_{1y}.

$$10^6 \times \begin{pmatrix} 66.0 \\ 83.9 \end{pmatrix} = 10^{11} \times \begin{pmatrix} 2.9813 & -1.2039 \\ -1.2039 & 2.2844 \end{pmatrix} \begin{pmatrix} u_{1x} \\ u_{1y} \end{pmatrix} \quad (9)$$

u_{1x} and u_{1y} was found to be 0.47×10^{-3} m and 0.61×10^{-3} m respectively. Then to determine the magnitude of forces at node 2, we can substitute the values we obtain to the matrix equation (8). We find:

$$\mathbf{f} = 10^{11} \times \begin{pmatrix} 2.9813 & -1.2039 & -0.4928 & 0.6783 & -2.4885 & 0.5255 \\ -1.2039 & 2.2844 & 0.8493 & -1.8166 & 0.3546 & -0.4678 \\ -0.4928 & 0.8493 & 0.9050 & -1.8166 & -0.4122 & -0.9622 \\ 0.6783 & -1.8166 & 0.1129 & 0.1129 & -0.7913 & -0.7028 \\ -2.4885 & 0.3546 & -0.4122 & -0.4122 & 2.9007 & 0.4367 \\ 0.5255 & -0.4678 & -0.9622 & -0.9622 & 0.4367 & 1.1706 \end{pmatrix} \begin{pmatrix} 0.47 \times 10^{-3} \\ 0.61 \times 10^{-3} \\ 0 \\ 0 \\ 0 \\ 0 \end{pmatrix} \text{N/m} \quad (10)$$

By multiplying the right hand side of equation (9) we find the full form of the force matrix:

$$\mathbf{f} = 10^6 \begin{pmatrix} 66 \\ 83.9 \\ 29.1 \\ -79.8 \\ -94.9 \\ -41.1 \end{pmatrix} \text{N/m} \quad (11)$$

Finally, we obtain the magnitude of forces at node 2 using this equation:

$$F = \sqrt{f_x^2 + f_y^2} \quad (12)$$

We find that the force magnitude at node 2 is 84.9×10^6N/m.

4. Since we know the distribution of mass of the system and the stiffness matrix. To find the natural frequencies of the system, first we can start from the equation of motion (EOM):

$$\boldsymbol{M}\ddot{\boldsymbol{u}}(t) + \boldsymbol{C}\dot{\boldsymbol{u}}(t) + \boldsymbol{K}\boldsymbol{u}(t) = 0 \tag{13}$$

Where $\boldsymbol{M}$ is the mass matrix, $\boldsymbol{C}$ is damping matrix, $\boldsymbol{K}$ is stiffness matrix, t is time in Seconds, $\boldsymbol{u}(t)$ is nodal displacement with respect to time ($\dot{\boldsymbol{u}}$ is the first derivative and $\ddot{\boldsymbol{u}}$ is the second derivative).
Since material damping is negligible, the equation reduces to:

$$\boldsymbol{M}\ddot{\boldsymbol{u}}(t) + \boldsymbol{K}\boldsymbol{u}(t) = 0 \tag{14}$$

Then we find the free vibration of the system assuming that:

$$\boldsymbol{u}(t) = \boldsymbol{a}\cos(\omega t + \phi) \tag{15}$$

Where $\boldsymbol{a}$ is the displacement amplitudes matrix and ω is the natural frequency and ϕ is the phase angle. To solve the EOM we differentiate equation (15) twice and we get:

$$\ddot{\boldsymbol{u}}(t) = \boldsymbol{a}\cos(\omega t + \phi) \tag{16}$$

Substituting (15) and (16) to (14) and dividing by $\cos(\omega t + \phi)$ we get:

$$(\boldsymbol{K} - \omega^2\boldsymbol{M})\boldsymbol{a} = \boldsymbol{0} \tag{17}$$

Which is an eigenvalue problem. We can express it as:

$$(\boldsymbol{M}^{-1}\boldsymbol{K} - \omega^2)\boldsymbol{a} = \boldsymbol{0} \tag{18}$$

Comparing this with:

$$A\boldsymbol{v} = \lambda\boldsymbol{v} \tag{19}$$

The solutions to (17) are the eigenvalues $\lambda_i = \omega_i^2$, with eigenvectors $\boldsymbol{v_i} = \boldsymbol{a_i}$ for $i = 1,2$.
Therefore, we can find the determinant $(\boldsymbol{K} - \omega^2\boldsymbol{M}) = \boldsymbol{0}$

$$|\boldsymbol{K} - \omega^2\boldsymbol{M}| = \boldsymbol{0} \tag{20}$$

This matrix equation will give a polynomial equation of the order equal to the system D-O-F, which can then be solved to find the natural frequencies of the system ω_i where $i = 1,2,\ldots$n, n is the number of D-O-F.

References

1. Harry Coules & Alexander Velichko, 07/11/2022, MENG 30011 Applied Solid Mechanics, AY 2022/23 coursework assessment, University of Bristol.

Part C: Failure of Materials

Question 1

Q1a. Smallest number of strain measurement to determine σ_x and σ_y

Ans: 3 measurements

Q1b. Calculate applied stresses σ_x and σ_y from strain measurements

Ans:

1) The orientations of the strain gauges are 0, 45 and 90 degrees.

2) Table 1: Material properties of a large plate with rectangular cross-section.

Elastic modulus (E)	70 GPa
Poisson's ratio (v)	0.3
Yield strength (σ_Y)	400 MPa
Fracture toughness (K_{IC})	20 MPa $\sqrt{\text{m}}$

The applied stresses are found using Hooke's Law. Since it is a large plate with rectangular cross-section, it was assumed to be in plane stress. Therefore, stresses normal to the z-axis is zero. Normal stresses in the x and y direction were obtained using equation (1) and (2):

$$\sigma_x = \frac{E}{(1-v^2)}(\sigma_x + v\varepsilon_y) \quad (1)$$

$$\sigma_y = \frac{E}{(1-v^2)}(\sigma_y + v\varepsilon_x) \quad (2)$$

ε_x and ε_y was obtained from the MATLAB code with the values of -0.0013 and 0.0021 respectively.

Hence, it was found that the values of $\sigma_x$and σ_y are -51.54 MPa and 131.5 MPa respectively.

Q1c. Analysis of possible failure mechanisms

There are two possible failure mechanisms: ductile or brittle fracture.

We assume that the component is in plane stress therefore it only experiences stress in x and y direction. All the relevant material properties used in the analysis can be found in Table 1.

First, we need to obtain the new stress tensor with the additional stress σ_P, which is applied at θ =30° measured from the x axis. The rotated stress tensor can be obtained from equation (3)

$$\boldsymbol{\sigma'} = \boldsymbol{\sigma_r} \cdot \boldsymbol{\sigma_i} \cdot \boldsymbol{\sigma_r^T} = \begin{pmatrix} cos(\theta) & sin(\theta) \\ -sin(\theta) & cos(\theta) \end{pmatrix} \begin{pmatrix} \sigma_{xx} & \tau_{xy} \\ \tau_{xy} & \sigma_{yy} \end{pmatrix} \begin{pmatrix} cos(\theta) & -sin(\theta) \\ sin(\theta) & cos(\theta) \end{pmatrix} \quad (3)$$

Where $\boldsymbol{\sigma_r}$ is the rotation tensor and $\boldsymbol{\sigma_i}$ is the initial stress tensor.

We then obtain the new stress tensor $\boldsymbol{\sigma_{new}}$ by adding the additional stress to σ_{xx}.

$$\boldsymbol{\sigma_{new}} = \boldsymbol{\sigma'} + \begin{pmatrix} \sigma_p & 0 \\ 0 & 0 \end{pmatrix} \tag{4}$$

From the new stress tensor, we can obtain the principal stresses.

$$\sigma_{1,2} = \frac{\sigma_{11} + \sigma_{22}}{2} \pm \sqrt{\left(\frac{\sigma_{11} - \sigma_{22}}{2}\right)^2 + \sigma_{12}^2} \tag{5}$$

First, we consider ductile failure caused by yielding due to stresses.

We obtain Tresca or Von Mises equivalent stress by plugging in the principal stresses.

$$\sigma_{Tresca} = max(|\sigma_1 - \sigma_2|, |\sigma_1|, |\sigma_2|) \tag{6}$$

$$\sigma_{VM} = \sqrt{\frac{(\sigma_1 - \sigma_2)^2 + \sigma_1^2 + \sigma_2^2}{2}} \tag{7}$$

To obtain safety factor, we plug in corresponding equivalent stresses.

$$SF = \frac{\sigma_Y}{\bar{\sigma}} \tag{8}$$

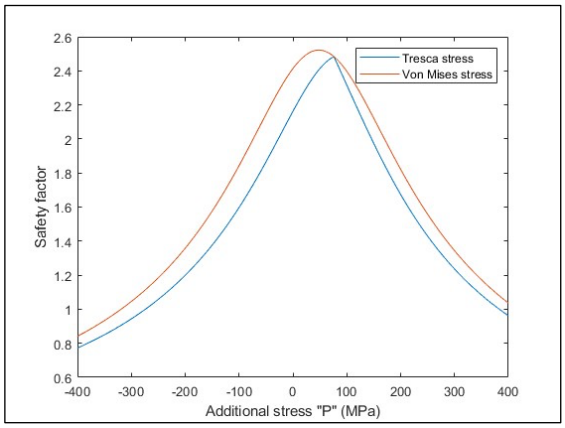

Figure 4 Plot of safety factor against additional stress P

Figure (1) shows the corresponding safety factor when additional stress $|\sigma_p| \leq 400$ MPa is applied. Using yield criterion where $\bar{\sigma}=\sigma_Y$, we obtain the range of σ_p where it is considered safe against yielding.

Table 5: Range of 'safe' stress value (negative sign indicates stress is compressive, positive sign indicates stress in tensile)

Von Mises Equivalent Stress	σ_p > -274 MPa
Tresca Equivalent Stress	-321 < σ_p< 383 MPa

Next, we consider brittle failure caused by crack. It is assumed that a central crack of arbitrary orientations can propagate due to environmental and loading conditions. For brittle failure, safety factor can be obtained from equation (9).

$$SF = \frac{K_{IC}}{K_I} \tag{9}$$

First, we need to obtain stress intensity function (K_I), which is the function of applied load and crack length.

$$K_I = Y\sigma_D\sqrt{\pi a} \tag{10}$$

Since it is a central crack, then geometry correction factor Y is equal to 1, a is the crack length where it is 2.5 mm, since 2a = 5 mm, the minimum detectable crack length by the NDT equipment, and σ_D is design stress in MPa. σ_D is obtained from σ_{yy} of the new rotated stress tensor, as the stress propagating the crack growth is normal to σ_{yy} and the load is assumed to be Mode 1. 181 x 801 cell arrays was produced in MATLAB, containing values of σ_D by iterating for $|\sigma_p| \leq 400$ MPa and $0° \leq \theta \leq 180°$.

When K_I reaches fracture toughness (K_{IC}), then fracture occurs, as safety factor is below 1. By obtaining stress intensity factor (K_I) corresponding to $|\sigma_p| \leq 400$ MPa for $0° \leq \theta \leq 180°$, we can observe at which orientation and stress value the component reaches fracture.

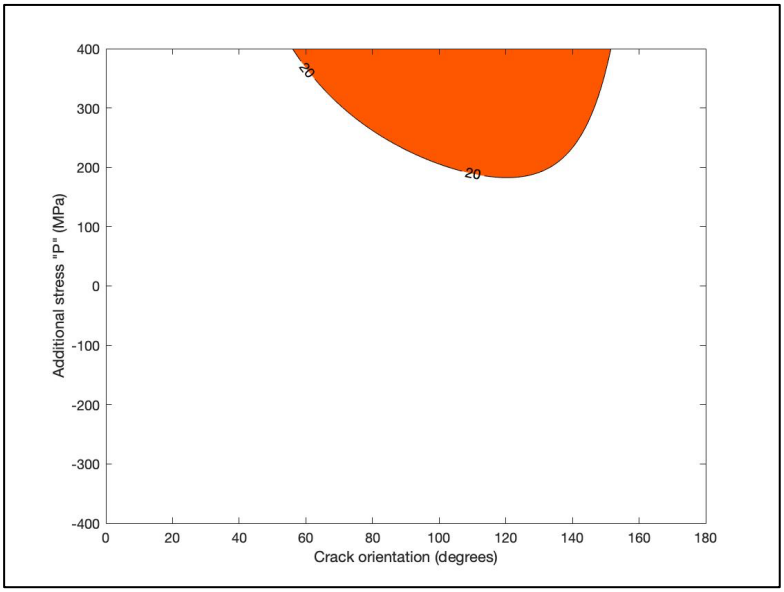

Figure 2 2D contour plot for stress intensity factor corresponding to additional stresses at each crack orientations

The orange region indicates the corresponding σ_p and θ where fracture will occurs, the white region indicate the safe region for corresponding σ_p and θ for the crack to not cause fracture. Note that only tensile stress contributes to propagating the crack growth, therefore all compressive stresses results in zero stress intensity factor.

It is assumed that stress intensity factor (K_I) satisfies Linear Elastic Fracture Mechanics (LEFM). To check if LEFM is valid, equation (11) is used.

$$\frac{4}{\pi}\left(\frac{K_I}{\sigma_Y}\right)^2 \leq a \tag{11}$$

Where a is 2.5 mm.

Values that doesn't satisfy LEFM implies that plastic zone is significant to the crack size, therefore Elastic-Plastic Fracture Mechanics (EPFM) approach needs to be used. Therefore, we can use Irwin's correction using equation (12).

$$K_{eff} = \frac{K_I}{\sqrt{1 - \frac{1}{2}\left(\frac{\sigma_D}{\sigma_Y}\right)}} \tag{12}$$

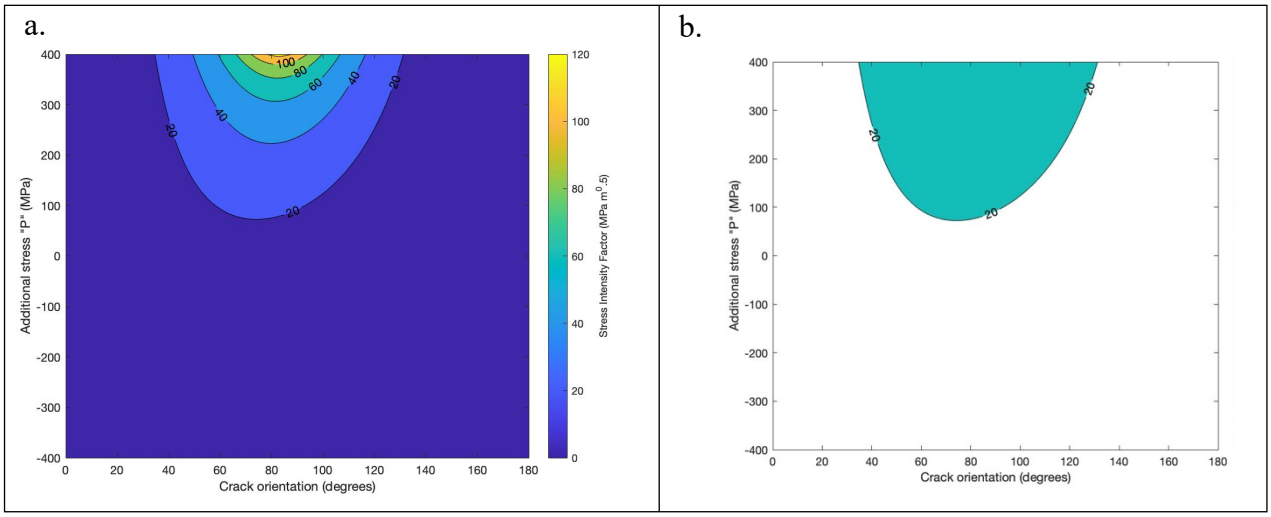

Figure 6 a.) Effective K value after Irwin's correction b.) Effective K value above K_c

Figure 3(a) shows the stress intensity factor after Irwin's correction and figure 3(a) shows the value for which the corresponding additional stress and crack orientation will cause fracture at the green region where K reaches above fracture toughness. **It was found from the contour plot that the most dangerous orientation of the crack is around 73°-77° as it will already reach fracture at a low σ_p of 63 MPa. From the analysis, it was concluded that the σ_p that will not cause failure is ranging from -321 MPa, obtained from safety factor using Tresca equivalent stress until 63 MPa, where it reaches brittle failure at the most dangerous orientation.**

Q2a. How probability of failure depends on inspection interval

We first consider two possible failure mechanism; leak-before-fracture or fatigue. We can determine the failure mechanism by obtaining crack length at failure a_f. We can obtain this using equation (13) below.

$$K_I = K_{IC} = Y\sigma_{max}\sqrt{\pi a_f}. \tag{13}$$

Where fracture toughness (K_{IC}) is 90 MPa$\sqrt{\text{m}}$, Y is geometry correction factor, σ_{max} is the maximum stress acting on the plate which is the axial stress, since it is normal to the crack. It is assumed to be a central crack on infinite plate, so Y=1.

We first need to determine the principal stresses:

$$\sigma_\theta = \frac{pR}{t} \tag{14}$$

$$\sigma_{axial} = \frac{pR}{2t} \tag{15}$$

$$\sigma_r = p \tag{16}$$

Where p is the internal pressure which is 40 MPa at cyclic loading and 80 MPa for short-term rise, R is the outer radius of the pipe which is 100 mm, and t is the thickness of the pipe which is 10 mm. Since $R \gg t$, then σ_r is negligible.

We can now obtain a_f using equation below:

$$a_f = \frac{1}{\pi}\left(\frac{K_{IC}}{Y\sigma_{axial}}\right)^2 \tag{17}$$

We then obtain a_f for both cyclic loading and during short-term rise where we obtain 64.5 and 16.1 (in mm) respectively. Since in both cases $a_f >$ t, then **leak-before-fracture** will occur.

First, we assume that the probability of failure is the probability of not detecting a crack, where we can obtain from 1 – $P_{pod}(a)$ from the given MATLAB code. Therefore, the probability is failure is a function of crack length which can be from the plot below:

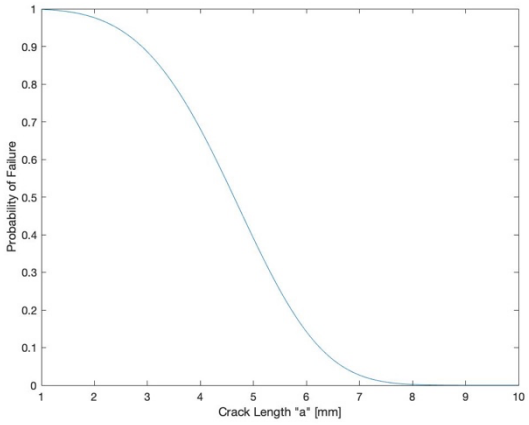

Now we consider the inspection interval effect on probability of failure. First, we need to find the growth rate of crack. We can obtain this using equations below:

$$\frac{da}{dN} = C(\Delta K)^m \tag{18}$$

$$\Delta K = Y\Delta\sigma\sqrt{\pi a} \tag{19}$$

$$Y = 0.278 + 0.373\left(\frac{a}{t}\right)^2 - 0.029\left(\frac{a}{t}\right)^4 \tag{20}$$

Where C is the fatigue crack growth which is $10^{-12}\,\frac{\mathrm{m/cycle}}{(\mathrm{MPa}\sqrt{\mathrm{m}})^m}$ where m=4.

We assume that the initial crack length is at 1 mm, and crack length at failure is equal to thickness which is 10 mm.

From this, we can obtain the number of cycles (N) for crack to go from initial size to failure. We can obtain N by equation below:

$$N = \int_{ai}^{af} \left(\frac{dN}{da}\right) da = \int_{ai}^{af} \frac{da}{C\left(Y\Delta\sigma\sqrt{\pi a}\right)^{m}} \tag{21}$$

It was found that it takes about 174000 cycles for the crack to grow until failure. The inspection interval was then determined by iterating the range until it corresponds to probability of failure of 0.01.

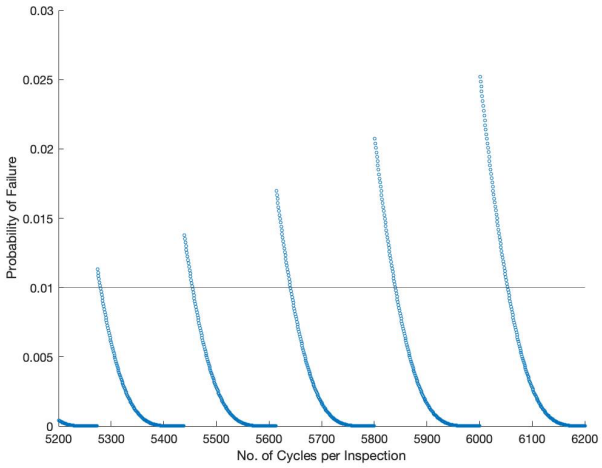

Figure 7 Probability of failure vs. inspection interval

Figure (7) shows the probability of failure corresponding to inspection interval that is number of cycles per interval. It was found from the analysis that the probability of failure depends on the interval between inspections done as the probability of failure is probability of crack being undetected after every inspection during its operation life.

Q2b. Inspection interval where P_{pof} = 0.01

The minimum number of inspection interval that corresponds to probability of failure at 0.01 is between **5279 and 5280**, this was obtained from figure 7, at which the line first intersects at 0.01 probability of failure.

References

1. Harry Coules & Alexander Velichko, 07/11/2022, MENG 30011 Applied Solid Mechanics, AY 2022/23 coursework assessment, University of Bristol.

2. Moler, C. (1970) "MATLAB," MathWorks. Simulink. Available at: https://www.mathworks.com/products/matlab.html (Accessed: December 15, 2022).